IEEE Access
Multidisciplinary | Rapid Review | Open Access Journal

Received October 29, 2017, accepted January 30, 2018, date of publication February 9, 2018, date of current version March 16, 2018.

Digital Object Identifier 10.1109/ACCESS.2018.2804378

A Portable Live-Cell Imaging System With an Invert-Upright-Convertible Architecture and a Mini-Bioreactor for Long-Term Simultaneous Cell Imaging, Chemical Sensing, and Electrophysiological Recording

DHANESH KATTIPPARAMBIL RAJAN[1], (Student Member, IEEE), JOOSE KREUTZER[1], HANNU VÄLIMÄKI[1], MARI PEKKANEN-MATTILA[2], ANTTI AHOLA[1], ANNE SKOGBERG[1], KATRIINA AALTO-SETÄLÄ[2,3], HEIMO IHALAINEN[1], PASI KALLIO[1], AND JUKKA LEKKALA[1]

[1]BioMediTech Institute and Faculty of Biomedical Sciences and Engineering, Tampere University of Technology, FI-33720 Tampere, Finland
[2]BioMediTech, Faculty of Medicine and Life Sciences, University of Tampere, FI-33100 Tampere, Finland
[3]Heart Hospital, Tampere University Hospital, FI-33521 Tampere, Finland

Corresponding author: Dhanesh Kattipparambil Rajan (dhanesh.kr@tut.fi)

This work was supported by the Finnish Funding Agency for Technology and Innovation (TEKES) through Human Spare Parts 2 Project under Grant 40332/14.

ABSTRACT Cell culture *in-vitro* is a well-known method to develop cell and disease models for studying physiologically relevant mechanisms and responses for various applications in life sciences. Conventional methods for instance, using static culture flasks or well plates, have limitations, as these cannot provide accurate tractable models for advanced studies. However, microscale systems can overcome this since they mimic the cells' natural microenvironment adequately. We have developed a portable live-cell imaging system with an invert-upright-convertible architecture and a mini-bioreactor for long-term simultaneous cell imaging and analysis, chemical sensing and electrophysiological recording. Our system integrates biocompatible cell-friendly materials with modular measurement schemes and precise environment control and can be automated. High quality time-lapse cell imaging is hugely useful in cell/disease models. However, integration of advanced *in-vitro* systems into benchtop microscopes for *in-situ* imaging is tricky and challenging. This is especially true with device based biological systems, such as lab/organ/body-on-chips, or mini-bioreactors/microfluidic systems. They face issues ranging from optical and physical geometry incompatibilities to difficulties in connectivity of flow and perfusion systems. However, the novel modular system we have developed either as an inverted or as an upright system can easily accommodate virtually any *in-vitro* devices. Furthermore, it can accept additional sensor or measurement devices quite freely. Cell characterization, differentiation, chemical sensing, drug screening, microelectrode-array-electrophysiological recordings, and cell stimulation can be carried out with simultaneous *in-situ* imaging and analysis. Moreover, our system can be configured to capture images from regions that are otherwise inaccessible by conventional microscopes, for example, cells cultured on physical or biochemical sensor systems. We demonstrate the system for video-based beating analysis of cardiomyocytes, cell orientation analysis on nanocellulose, and simultaneous long-term *in-situ* microscopy with pO_2 and temperature sensing. The compact microscope as such is comparable to standard phase-contrast-microscopes without any detectable aberrations and is useful practically for any *in-situ* microscopy demands.

INDEX TERMS Portable compact microscope, label-free long-term live-cell imaging, modular portable microscope for *in-situ in-vitro* cell imaging, portable cell culture system, portable cell culture and measurement system, low-cost biosensor technology.

I. INTRODUCTION

Live-cell microscopy is a tool used commonly in various research applications and, is instrumental in investigating numerous intra and extra cellular dynamic processes and their environmental interactions. Traditional approaches to live-cell imaging are often based on short or long- term time-lapse microscopy (TLM) using high quality biological microscopes [1], [2]. The growing interest in this area is perhaps best evidenced by the dramatic increase in the number of papers reporting numerous TLM studies in life sciences. In most TLMs, the cellular activity is imaged for durations ranging from milliseconds to hours in a specimen chamber with special environment control [3], [4]. A TLM system for biological specimens is typically equipped with a contrast enhancement technique such as, differential interference contrast (DIC) or Hoffman modulation contrast (HMC), or fluorescence or phase contrast [1]. They can capture images at defined time points to produce a TLM montage or movie to unveil dynamic biological processes. High-end systems coupled with dedicated TLM softwares often support high frame rate movie recordings, and if desired, timely analysis of captured images during the TLM. The State-of-the-art TLM systems employ imaging modalities such as confocal and super resolution procedures in order to improve the contrast, to reduce the photo-cytotoxicity and to capture images at resolutions higher than Abbe's classical diffraction-limited resolution [5]. The quality of TLM images by these systems is high, however, it comes with a price; high costs and often the hardware involves fairly complicated settings with large form factors and high upkeep [6]. These systems oftentimes cannot satisfy the need for high throughput observations due to their bulky volume and limited flexibility [7]. Besides, in several device based biological systems, for example, lab/organ/body-on-chips, reaction chambers, bioreactors, and microfluidic culture systems, the real time processes need to be timely imaged in *in-situ*. They can experience tremendous challenges while being embedded into an off-the-shelf TLM system, due to issues ranging from optical and physical geometry incompatibility to difficulties in connectivity of flow and perfusion systems [8]–[17]. Several recent developments in physical, chemical and biological sensors for cell culturing and cellular-tissue models are steadily being integrated into systems for drug screening, regenerative medicine and stem cell engineering [18]–[20]. These sensors are efficient candidates for process monitoring and environment regulation, however, most of them, unfortunately, are not compatible with conventional TLM hardware for synchronised imaging. Despite various TLM systems with remarkable specifications being continually available in the market, still adapting steadily developing technologies into them is difficult and laborious.

Breaking the barriers of achievable spatial resolution in microscopy is obviously important, but at the same time, the demand for miniaturized versions of biological microscopes with uncompromising imaging quality is also continually increasing. Compact microscopes instead of high-end, large-form-factor microscopes, are unavoidable in several instances, for obvious reasons, like following the biological events *in-situ* in real time inside or outside of an incubator. Over the last years, several compact microscopes, have been developed and some have been commercialised [21], [22]. A number of compact systems, based on the emerging microscope modalities have been reported recently. The on-chip brightfield - fluorescent microscopes [23]–[26] have successfully demonstrated high resolution, large field-of-view (FOV) and incubator compatibility. However, the cells need to be plated on the imaging chip, making them less attractive for conventional cell culturing workflow. On the contrary, digital holographic microscopy (DHM) is an excellent choice for widefield lensless 2D/3D imaging, and numerous compact systems have been recently reported [27]–[29]. DHM, in general, can be implemented as a shadow or fluorescent imaging modality either by quantitative or qualitative means, but in all cases, the image of the object must be reconstructed numerically from the diffraction pattern of the specimen recorded [30], [31]. DHM, being a computational microscopy, thus typically lacks the immediate visualization of the specimen, which can be cumbersome in certain biomedical procedures [32]. Another imaging modality – the optical projection tomography, that developed notably in the last decade can produce 3D cell images, but apparently is not directly suitable for live-cell imaging. On the other hand, nonlinear optical imaging methods are suitable for live-cell imaging, but the miniaturization – from the instrumentation point of view- is tricky. On the contrary, fiber optic microscopy has remarkable advantages, but integrating fibers into cell chambers can be sometimes severely chaotic [33]–[38]. In addition to downsizing the newly emerging microscope modalities, modifying existing microscopy modalities to construct portable compact microscopes have unprecedented potential, especially when they are equipped with features for wireless communication, web interfacing and smart phone compatibility. They can have widespread applications in remote cell microscopy, mobile healthcare and on-field medical diagnosis [39], [40]. Though several compact microscopes have been reported, most of them, except for a few are either bright-field or fluorescent systems [23]–[26], [39]–[41]. As live-cells are highly transparent for visible wavelengths, the image contrast is extremely poor in bright-field systems. The contrast is greater in fluorescent systems, but staining with fluorescent markers is inevitable, which can sometimes be toxic and unacceptable. While chromatic aberration is visible in some of the reported cost-effective systems [7], controlling all the camera features in webcam based systems is not straight-forward or is sometimes impossible [7], [42], [43]. Besides, the maximum frame rate in web-cam systems might be insufficient for fast dynamic recordings.

Almost all the compact microscopes reported are intended to be used with a specific system or for a specific purpose and not necessarily modular for extended applications. They have been explicitly designed to be used either in the inverted or in

the upright configuration and are mutually exclusive. In this context, we present a compact portable live-cell imaging system with a novel modular architecture, configurable either as an inverted or as an upright system, and with a mini bioreactor for simultaneous long-term live-cell imaging, chemical sensing and electrophysiological recording. The system consists of a digital microscope module, an illumination module, positioning and a motorized focusing stage, mini-incubator with biocompatible and cell-friendly materials, fluorometric pO_2 sensor and microelectrode array (MEA) amplifier. We put forward a design where the illumination and microscope modules can be swapped, i.e. the system can be converted between inverted and upright configurations. This architecture enables the system to be useful not only for conventional inverted spatiotemporal cell imaging, but also as an upright system when the room below the cell platform is unavailable for inverted microscopy. When sensors such as opto-chemical sensors [18], [19] need to be integrated into cell platforms, ideally, they must operate in close proximity of the cells, i.e typically just under the cell platform, and resultantly, simultaneous uninterrupted inverted microscopy is practically impossible. In our design, the system can then be switched into an upright configuration, therefore, biochemical measurements conjointly with live-cell imaging becomes possible. The microscope module consists of mainly three optical components - a machine vision camera, a mirror cube and a phase contrast objective. The illumination module comprises primarily of a white LED, a LED lens, a ground glass diffuser and a projection lens. It provides a stable and reasonably safe illumination in bright-field or dark-field or phase contrast schemes. The manual xyz-stage module enables sample xy-positioning and coarse focusing. Fine focusing is accomplished with a motorized linear stage. The magnification can be adjusted, primarily by changing the objective lenses and additionally by using lensless extension tubes. We employ highly corrected phase contrast objectives to produce high quality cell images with minimal halo, distortion and aberration. The bioreactor assembly comprises of a transparent ITO cell heater, a mini-incubator with polydimethylsiloxane (PDMS) cell chamber [44], [45] and gas supply for CO_2 buffering.

In the following, we first present a detailed construction of the developed modular microscopy system. Then the microscopy characterization and system performance results, based on studies with a resolution test-target and stained histology specimens, are shown. In the live-cell microscopy section, we study the system performance in different configurations when imaging a set of unstained cells. Then we show the results from orientation analysis of fibroblasts, long term video-based beating analysis of cardiomyocytes and an excerpt from simultaneous pO_2 sensing and TLM study. We complete the paper by experimenting the z-stack capabilities of the system and, finally we discuss the results.

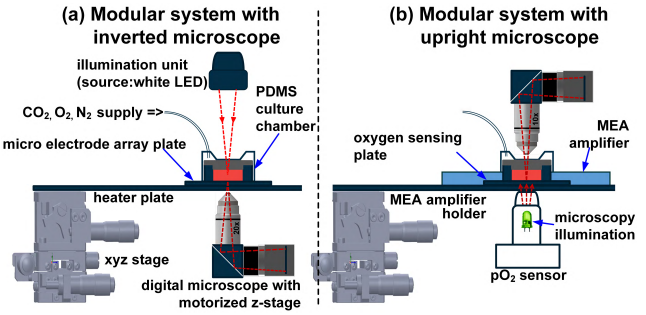

FIGURE 1. Modular microscopy schematic arrangement for (a) inverted microscopy and (b) upright microscopy with optical fluorometric oxygen sensor and MEA amplifier.

II. MODULAR CELL CULTURING SYSTEM ASSEMBLY

The modular system is schemed in FIGURE 1. The whole system was designed utilizing 3D computer-aided design (CAD) in Solidworks®. Firstly, the 3D models of suitable commercially available opto-mechanical parts were imported into the design, and the remaining parts were custom designed (anodised aluminium). The sub-assemblies of the final interchangeable assembly (see FIGURE 2) are: a camera module, an illumination module, a manual xyz-stage module, a motorized focus stage, PDMS mini-incubator, pO_2 sensor as well as a MEA amplifier with its holder. An original photograph of the final assembly is shown in FIGURE 2e. The details of each module are separately described in the following paragraphs. Check the supplementary materials section for system design CAD files.

A. CAMERA MODULE

A high quality digital microscope is constructed using an achromat phase contrast objective, a mirror cube (CCM1-E02/M-Thorlabs) and a machine vision camera. The microscope assembly is illustrated in FIGURE 3a. Two adapters (SM1A10-Thorlabs) and a coupler (CMT2-Thorlabs) are used for coupling the parts in the assembly. A camera with internal C or CS mount in the front aperture is required in the design. In the experiments discussed later, monochrome (>40 frames-per-second) or colour camera was used depending on the nature of application and intended analysis. The machine vision camera and the objective lens are mounted perpendicular to each other through the mirror cube. This geometry keeps the digital microscope very compact and facilitates a fixed mounting hole for objectives in the imaging plane. Moreover, it provides a great deal of space perpendicular to the imaging plane for additional optics. The mirror cube can be locked in its holder (FIGURE 2), either in upward or downward direction, respectively for inverted or upright microscopy. The cube holder's rail carrier head (dovetail RC2-Thorlabs, FIGURE 2a) allows upward or downward wobble-free translation of the holder and allows to lock it securely at any place along the length of the corresponding dovetail rail (RLA1200-Thorlabs, FIGURE 2a). Further, with this mechanism, the camera

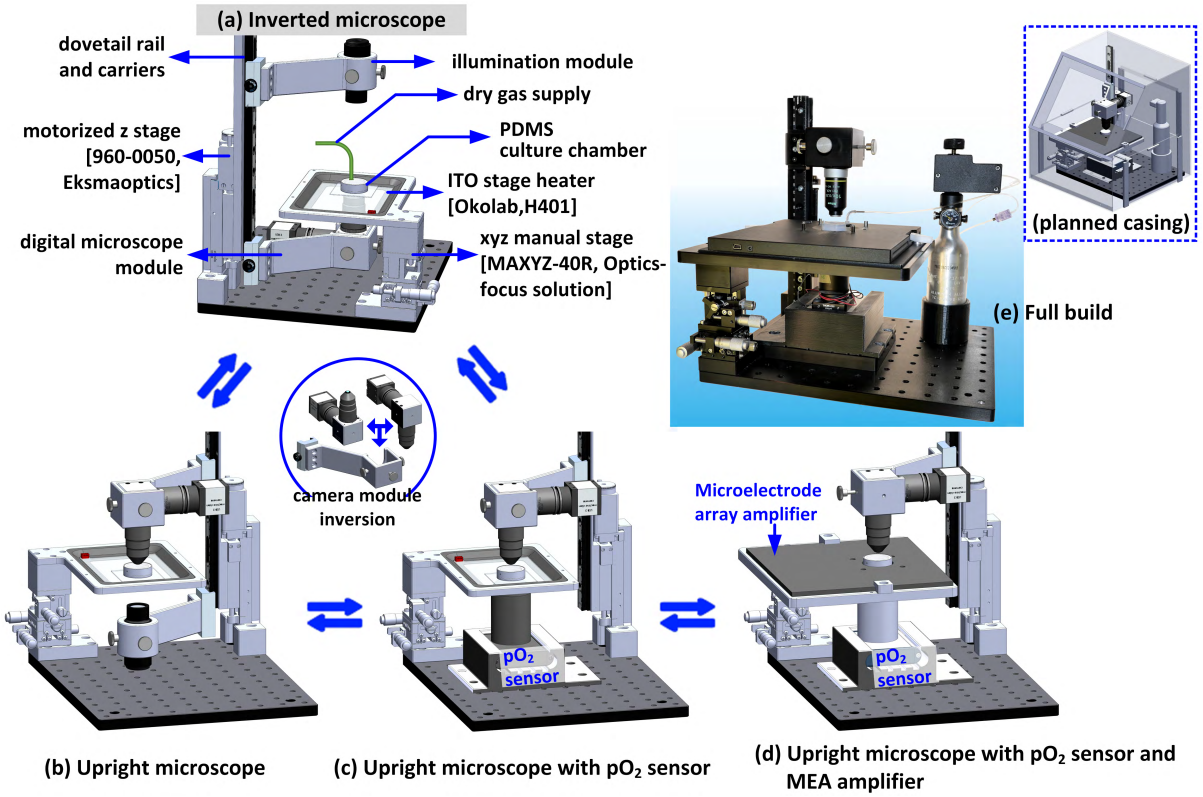

FIGURE 2. Modular system in different configurations. Microscope assembly for (a) inverted configuration and (b) upright configuration. (c) Upright configuration with oxygen sensor. (d) Upright configuration with MEA amplifier (MEA1060-Up, Multichannel System) and oxygen sensor. (e) Original photograph of the final assembly.

module can be easily taken out or snapped onto the rail anywhere along its length, even without accessing the rail ends.

B. OBJECTIVES

We utilize phase contrast objectives (Nikon CFI Achromat ADL 10XF, 20XF and 40XF) to produce cell images with unsurpassed details with little or negligible phase contrast halo. These objectives, in principle, transform the differences in the relative phase between the surround-un-deviated wave and the diffracted wave (by the specimen) into amplitude differences in the image [46]. An appropriate illumination (light manipulation through an annular ring) and objective placement (keeping the objective phase plate in conjugate to the illumination annular ring) are essential to achieve the maximum contrast ratio. See section '*Illumination module*' for the details of our illumination arrangement. TABLE 1 in the experimental section shows the technical specifications (measured and formula calculated) corresponding to the implementation of the select objectives. In addition to using high magnification objectives, the overall system magnification for a select objective can be improved, to a certain extent, by mounting stackable extension tubes of varying lengths in the light path (FIGURE 3a). Extension tubes are lensless hollow cylinders that stay between the objective and the camera, causing the camera sensor to move further from the objective and focus more closely, which in turn increases the overall magnification. The extension distance divided by the objective lens's focal length ultimately decides the amount of overall magnification (see TABLE 1).

C. ILLUMINATION MODULE

The anatomy of the compact illumination module is illustrated in FIGURE 3b. It consists of two separate stackable sub-assemblies, where the bottom sub-assembly can be stacked onto the main-assembly with or without an appropriate annular ring suitable for dark-field or phase contrast scheme. The optical train of the main-assembly comprises of a LED (3w-cool white, spectrum ~410-750nm, LXHL-LW3C-Lumileds), a bowl-shaped PMMA-LED collimator lens (FA10696 LN2-RS-LEDiL), a ground glass diffuser (DG05-1500-MD-Thorlabs) and spacers (stainless steel retaining rings (SM1RR, SM1RRC-Thorlabs) and 3D printed ones). All components are packed in Ø1" lens tube (SM1M20). Components can be accessed from both ends of the lens tube. A threaded adapter (S1LEDM-Thorlabs) serves as the LED lock at the top of the tube, and helps one to replace the LED without disturbing other components in the main assembly. The other sub-assembly has just two optical components, a 3D printed condenser annular ring and a plano-convex lens (L12224/L8080/L11388-SurplusShed) enclosed in an adapter (AD15F-SM1-Thorlabs) in a 3D printed casing.

TABLE 1. Modular microscope optical performance specifications, measured and estimated in air (at wavelength 550nm).

Objective lens	Extension tube length (mm)	WD[Δ] (mm)	NA[†]	Resolution[σ] (μm)	DOF (μm)	Field of View (μm)	True magnification
10X	0	12.74	0.12	2.69	17.62	1580.25	4.54
"	15	12.20	0.13	2.58	16.18	1347.37	5.33
"	25	11.74	0.14	2.48	15.00	1219.05	5.89
"	40	11.41	0.14	2.42	14.18	1075.63	6.68
"	80	10.60	0.15	2.25	12.27	820.51	8.75
20X	0	5.91	0.22	1.55	5.80	691.89	10.38
"	15	5.61	0.23	1.47	5.24	600.94	11.95
"	40	5.48	0.23	1.44	5.01	490.42	14.64
40X	0	5.75	0.23	1.43	4.96	190.48	37.70
"	15	5.70	0.24	1.42	4.88	162.44	44.20

[Δ]WD=working distance, [†]NA=numerical aperture= ref.index*sin (tan^{-1}(aperture radius/WD)), [σ]Resolution = 0.61*wavelength/NA, DOF=depth of focus[55]

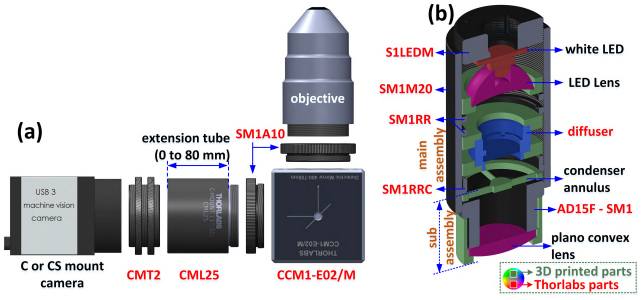

FIGURE 3. Compact microscopy parts. (a) Component assembly of the digital microscope. (b) anatomy of the illumination module. Here, the bottom sub-assembly is stackable onto the main assembly. This enables easy replacement of the condenser annule while the objective lens is changed. The S1LEDM-adapter functions as a lock for testing or replacing of LEDs (prefer star type or 5mm through hole-LEDs).

The diffuser in the light path is critical for a highly homogenous illumination for high contrast imaging. A diffuser with 1500 grits was specifically selected after several cell-imaging trials to accomplish the greatest possible contrast. The illumination module has a variable NA (0.08 - 0.27) and a matching annule needs to be inserted into the sub-assembly once the objective is changed. The illumination module to the specimen distance is adjusted freely to take full advantage of the NA.

D. STAGE MODULE AND MOTORIZED FOCUSING STAGE

A manual xyz-stage (MAXYZ-40R, Optics-focus solution, see FIGURE 2a) with micrometer head screws, is included in the set-up for coarse focusing and sample positioning (x, y $=$ $\pm$6.5mm, z $=$ 10mm, resolution $=$ 10 μm). A custom machined metallic frame with a rectangular slot is mounted onto the xyz-stage where, a standard k-frame transparent stage heater (Okolab, H401) can be loaded and locked. Once the camera and illumination modules are appropriately positioned on the dovetail rail and is coarsely focused, the motorized fine focusing is carried out from the software side. The narrow motorized translation stage (960-0050, Eksma Optics, see FIGURE 2a) enables fine focusing (z $=$ 50 mm, resolution $=$ 1.25 μm [full steps]) at a maximum speed of 5 mm/s. Furthermore, a specific stepper controller (980-0045-USB-Eksmaoptics), is also capable of dividing the full steps upto 1/256 step/div for sub-micron stack acquisitions. The mechanical limit switches on the translation stage establish reference positions with an accuracy of several motor steps and assists emergency stopping.

E. FLUOROMETRIC pO_2 SENSOR AND MEA AMPLIFIER

The pO_2 sensing is based on phase-fluorimetric detection, where oxygen sensitive dyes, such as platinum(II) octaethylporphyrinketone are embedded in a thin, gas permeable polymer film (polystyrene) and then the pO_2 sensitive phase difference between the fluorescence emission and excitation signal are read [47]. For this purpose, we applied a super critical angle read-out scheme based on an in-contact parabolic lens [18], which has a high emission collection efficiency and, moreover, facilitates efficient total internal reflection excitation. These features make the detection insensitive to biofouling or other optical changes in the sensing surface and, more importantly, greatly reduces the amount of optical power radiated into the cell culture chamber. In addition, the set-up leaves room for microscopy illumination in the centre of the cell chamber.

The MEA amplifier (bandwidth: 1Hz-3 kHz, gain: 100-5000) is suitable for 49 mm $\times$ 49 mm MEA plates with 8x8 grid configuration for multisite, parallel electrophysiological recording. When the amplifier lid is closed, the contact pins are pressed onto the MEA contact pads which establishes the signal connectivity. The selected MEA amplifier ensures very high signal-to-noise ratio since the amplifier electronics stays very close to the MEA plate. External ITO heater can be avoided in MEA measurements as its integrated heating element and temperature sensor serves the purpose. Electrophysiological measurements combined with morphological or chemical sensing or fluorescence readouts and multisite stimulations can be efficiently carried out in the modular system.

F. INTERCHANGING BETWEEN INVERT AND UPRIGHT MICROSCOPY CONFIGURATIONS

The procedures involved in changing the microscope from invert to upright scheme are illustrated in the FIGURE 2a-c. Firstly, the digital microscope mirror cube is reversed in the

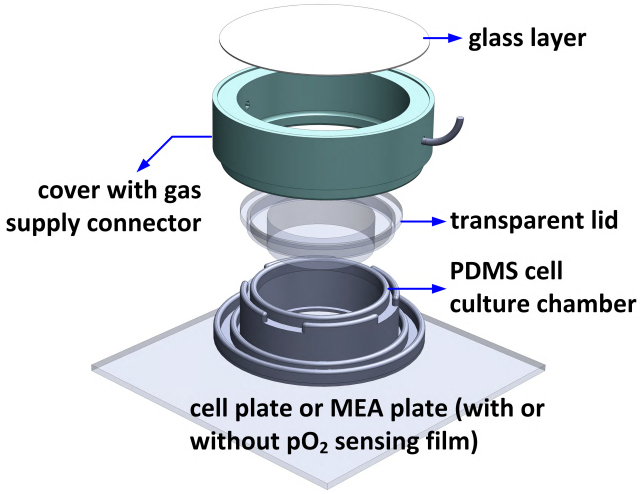

FIGURE 4. Schematic of the mini incubator that consists of PDMS cell culture chamber, transparent lid to seal the cell culture, and cover to enclose the environment to maintain the culture conditions utilizing dry gas supply from the side of the cover.

camera module and the illumination and camera modules are swapped vertically on the dovetail rail. Maintaining a gap of few mm between the objective and cell plate (or the outer layer of a culture chamber in upright microscopy) ensures safety and smooth motorized focusing. For upright microscopy, long working distance objectives are often necessary depending on the height of the culture chamber, which forces one to usually opt for low magnification objectives. In general, for most of the highly corrected series of plan fluorite and plan apochromatic-infinity objectives, the working distance decreases as both the magnification and numerical aperture increases. Therefore, out of the three objectives selected (TABLE 1), only 10X objective is particularly useful for upright microscopy where the cells are imaged from the top of the mini incubator having a height of 11mm. However, once the 10X objective is mounted, one can adjust the overall magnification by making use of extension tubes in the light path (TABLE 1).

III. MATERIALS AND METHODS

A. PDMS CULTURE CHAMBER (MINI INCUBATOR)

The schematic of the mini incubator is shown in FIGURE 4. A controlled gas supply (5% CO_2, 19% O_2, 76% N_2) during the long-term TLM is critical to maintain the pH of the culture medium for live and healthy specimens. The technique - providing gas supply surrounding the PDMS structure - is described previously [45] and is directly adapted here. Briefly, the structure of the cell culture device consists of three main parts: a cover, a lid, and a PDMS cell culture chamber. The cover and the lid were made from UV curable acrylic plastic (Shapeways, Eindhoven, The Netherlands) and polycarbonate (PC) (Saloteam Oy, Salo, Finland), respectively. The cell culture chamber was house–made and cast from PDMS (Sylgard 184, Dow Corning, USA) using standard soft–lithography techniques as explained in the previous study [44].

The lid seals the cell culture chamber watertight that prevents evaporation. The lid is highly transparent to facilitate a good optical path for microscopy. A small boss in the middle of the lid is immersed into the culture medium, which avoids empty space for water to condensate, and thus ensures undisturbed imaging during the entire TLM. The cover with glass window seals the environment around the cell culture chamber. A continuous supply (5ml/min) of dry gas mixture is provided (FIGURE 1, FIGURE 2) through the cover.

B. SOFTWARE INTERFACE AND CONTROL

Currently, a custom written Matlab (ver:R2016b)-UI (user interface) software is implemented for controlling the illumination, stage heater and time-lapse data logging (image or movie, sensors). A low-cost microcontroller (Arduino UNO R2) with a motor add-on board (Adafruit motor shield V2) enables controlling the LED illumination and focusing (stepper motor) translation stage. LED intensity can be regulated 0-100% (at 8-bit resolution) through a custom hardware-controlled LED dimmer using pulse-width-modulation (PWM) signal from Arduino. Matlab's image acquisition tool-box in conjunction with Arduino and PointGray third-party Matlab packages facilitate a two-way control of Arduino and PointGray machine vision cameras from the UI [48]–[50] During TLM, the camera is configured to write directly into the PC disk, either as independent images when slow temporal changes are monitored or directly as an uncompressed high fps (frames-per-second) movie when fast dynamics, for instance, cardiomyocyte beating, is captured. Check the supplementary materials section for an exemplary Matlab script for illumination, camera and motorized focusing control and time-lapse image or video acquisition.

C. CELL CULTURING

Fibroblast culture: All chemicals and supplements for fibroblast culture, including Dulbecco's modified eagle medium (DMEM) high glucose, w/o L-glutamine, w/o sodium pyruvate (Biowest, L0101), Dulbecco's phosphate buffered saline (PBS) w/o calcium, w/o magnesium (Biowest, L0615), Trypsin-EDTA 1x w/o Calcium, w/o Magnesium, w/phenol Red (Biowest, L0930), L-Glutamine 100x, 200 mM (Biowest, X0550), Fetal bovine serum (FBS) USA (Biowest S1520), Penicillin-streptomycin solution 100x (Biowest L0022) were purchased from VWR and used as received or reconstituted according to manufacturer's instructions. Mouse embryonic fibroblasts (MEF) originally obtained from Wolfgang H. Ziegler (Hannover medical school, Hannover, Germany) were cultured in DMEM high glucose medium supplemented with 10% (v/v) fetal bovine serum (FBS), 1% L-glutamine, 1% P/S (100 IU mL^{-1} penicillin, 100 μg mL^{-1} streptomycin) in a standard incubator. Cells were harvested using trypsin-EDTA treatment and counted using a Bruker's chamber. For the studies of MEF alignment on nanocellulose surfaces, cationic cellulose nanofibers (c-CNF) were produced and coated on cul-

ture plates. Production, surface preparation and alignment mechanism of c-CNF is described in more detail in [51]. Glass plates (49 × 49mm) and PDMS-well culture chambers were cleaned by several immersions in 70% ethanol before coatings. After mounting PDMS-well culture chambers on the sterilized plates, eight sample plates were coated with c-CNF as described in [51] and three plates without c-CNF were used as reference for alignment analysis. For each well, cell suspension was seeded in a density of approximately 1.5×10^5 cells/mL. After seeding, the MEFs were allowed to adhere in a standard cell-culturing incubator for 30 to 120 minutes before filling the PDMS-well with culture medium (1 mL). Filled PDMS-well culture plates were either directly imaged in our system or cells were allowed to adjust and proliferate up to 24 h in the incubator before imaging.

iPS-CM culture: Cardiomyocytes were derived from human iPS-cell line UTA.04602.WT as previously described in [52]. Glass plates were first sterilized with 70% ethanol and dried properly before the PDMS ring was applied to the plates creating the well for the cells, subsequent to which ăthe beating iPS-CM aggregates were plated. Plates were hydrophilized with FBS and coated with 0.1% gelatin type A (Sigma-Aldrich, St Louis, MO, USA). For each plate, 3-4 beating iPS-CM aggregates were plated. The iPS-CMs were cultured in KO-DMEM-media (Lonza, Basel, Switzerland) with 20% FBS (Lonza), 1% non-essential amino acids (NEAA) (Cambrex, East Rutherford, NJ), 2 mM Glutamax (Invitrogen, Carlsbad, CA) and 50 U/ml penicillin/streptomycin (Lonza). After plating, the iPS-CM aggregates were cultured in an incubator overnight before imaging (inverted/upright). In all prolonged cell culturing, the medium in the PDMS culture chamber was replaced (twice a week) by fresh medium.

D. CYTOSPECTRE CELL ORIENTATION ANALYSIS AND VIDEO BASED BEATING SIGNAL ANALYSIS

A spectral orientation analysis tool (CytoSpectre[1.2]) [53] was used to analyse the images and characterize the degree of alignment of the cells on the c-CNF compared to control surfaces. Cytospectre analyses the orientation and wavelength distributions by performing Fourier transform to estimate the power spectrum of an image and, based on the spectrum, computes parameter values describing, among others, the mean orientation and anisotropy. From this, the circular variance (CV) – the measure of the shape distribution – is computed to describe the degree of cell orientation. The value of CV can range from 0 (isotropy i.e. perfect alignment of all oriented structures along a single line) to 1 (lack of isotropy).

Cardiomyocyte mechanobiological function was assessed using video microscopy based contraction measurement [54]. It uses digital image correlation methods on consecutive video frames to calculate a velocity vector field, based on which a directional signal characterizing the beating is obtained.

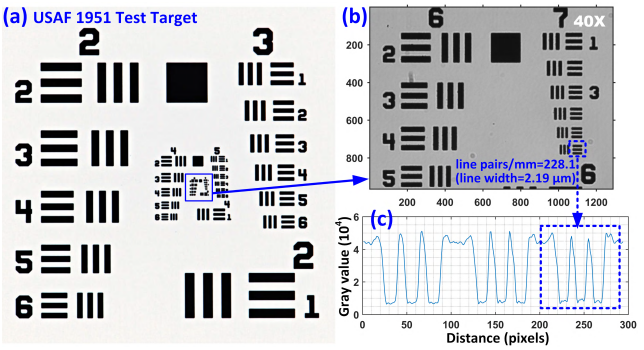

FIGURE 5. Microscopy characterisation. The USAF 1951 resolution test-target (a) original photograph and (b) microscopy image (40X, no extension tube). (c) intensity profile from three line groups ([4,7], [5,7], [6,7]). The dotted box corresponds to group [6,7] with 2.19 μm wide lines.

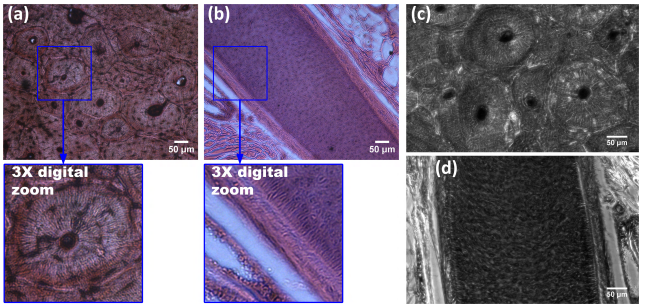

FIGURE 6. Modular microscope (inverted, 20X) images of stained histological samples. Human (a) hard bone grinding section and (b) skin section through hair follicle imaged using modular microscope. (c,d) reference images of the same samples with a benchtop-phase contrast microscope (Zeiss Axio observer z1).

IV. EXPERIMENTAL RESULTS

A. MICROSCOPY CHARACTERISATION

A standard positive resolution test-target (R1DS1P-Thorlabs) was used for measuring the resolution, FOV and true magnification. See FIGURE 5. for the example image of the resolution target captured with the 40x objective and a monochrome camera (PointGray, BFLY-U3-13S2M-CS, 1.3 MP, pixel size = 3.75 μm in 1/3" sensor). All the technical specifications for the three selected objectives with various extension tube lengths are summarised in TABLE 1. Because the objective lenses are implemented differently unlike in a recommended bench top microscope, the NA of the objectives had to be recalculated. We calculated this from the modified working distances.

B. PERFORMANCE COMPARISON WITH STAINED HISTOLOGICAL SAMPLES

Two stained human histological (Euromex PB.5221-Jaso Oy) specimens, 1) hard bone grinding section and 2) human skin section through a hair follicle were imaged with the proposed system (FIGURE 6a,b), and with a bench top biological phase contrast microscope for reference (FIGURE 6c,d). Microscopy images with the proposed system are notably comparable with the reference images, though the FOV and true magnification are slightly different in both the cases.

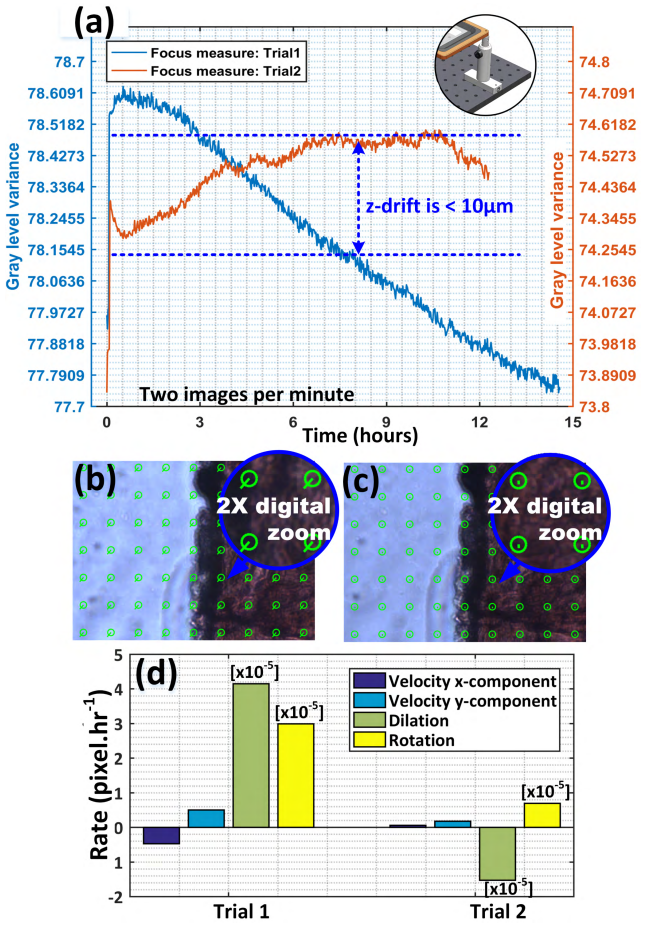

FIGURE 7. Long-term imaging performance measurements with a fixed specimen. (a) numerical estimation of focus [56]. Trial 1: measurement in room temperature. Trial 2: measurement at constant 37°C with a support pillar (inset). Ideally, a horizontal line would describe 0 focus drift. In our system, a slight focus drift is visible in Trial 2, but it is as low as 0.2% compared to 0.9% (Trial 1) in >12 hours period. (b, c) optical flow (overall relative physical movement of the specimen) in xy plane in Trial 1 and Trial 2 estimated as described in [57]. The flow vector (green line extending from the circles) indicates the xy movements were extremely small in Trial 2. (d) estimated flow field parameters [Note: -Vx indicates a shift of the last frame to the left compared to the first frame. Dilation and rotation quantify the overall expansion (or shrinking) and twisting (about z-axis) respectively of the measurement area].

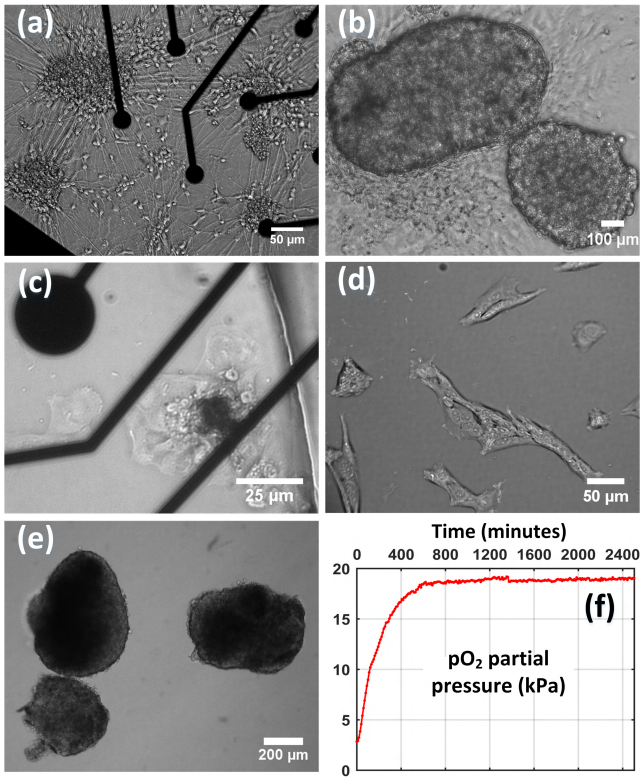

FIGURE 8. Modular microscopy images of live-cells captured on different occasions of corresponding cell culture. (a) neurons on micro electrode array (MEA) plate. (b,c) movie snapshots of a large and small (few cells) cluster of beating cardiomyocytes respectively on glass and MEA plate. (d) cropped view of MEF on glass. (e) beating cardiomyocytes on fluorescent pO_2 sensing film in simultaneous hypoxia and TLM study (upright configuration). (f) an excerpt from the corresponding pO_2 measurement log [18].

C. LONG-TERM PERFORMANCE AND STABILITY

In order to determine the focus consistency, TLM images (16 bit, 2 images/minute, camera: FL3-U3-13E4C-C) of the fixed specimen (FIGURE 6a) was captured for >12 hours and the focus was numerically computed (FIGURE 7a), as previously described in [56]. In Trial 1, images were captured at room temperature without ITO heating and the frame support pillar (FIGURE 7a inset). In Trial 2, the frame support was provided and the plate was set to 37°C for the whole duration. The mean focus drift is ∼0.9 % in Trial 1 but it is as low as only 0.2 % in Trial 2 in over 12 hours TLM. Additionally, the optical flow - the overall physical deformation between the first and last images in TLM image series - was estimated using Lucas-Kanade method based on the spatial and temporal image gradients [57]. In FIGURE 7b and FIGURE 7c the optical flow velocity vectors estimated are illustrated in corresponding images. Here, the green circles illustrate the points where the flow (movement) is computed, while the green lines represent the flow vector magnitude and direction. Additionally, the flow field parameters estimated are plotted in FIGURE 7d. Lucas-Kanade method is efficient to track apparent pixel translations in xy-plane which in turn helps to numerically estimate the xy drift of the imaging system. With a constant temperature supply and platform support, the x,y velocity components, though not zero, are much smaller (FIGURE 7d).

D. LIVE-CELL MICROSCOPY

Unstained living cells (neurons, fibroblasts and cardiomyocytes) were imaged independently on different occasions of cell culturing and the example snapshots are shown in (FIGURE 8). These trials were designed to iteratively fine-tune the optical performance of the microscopy module and, the suitability of the system for live-cell imaging was subsequently confirmed. The system, in different configurations, is reproducible and has been successfully utilized for long-term TLM observations. For example, the inverted configuration was implemented in order to study A) the alignment and

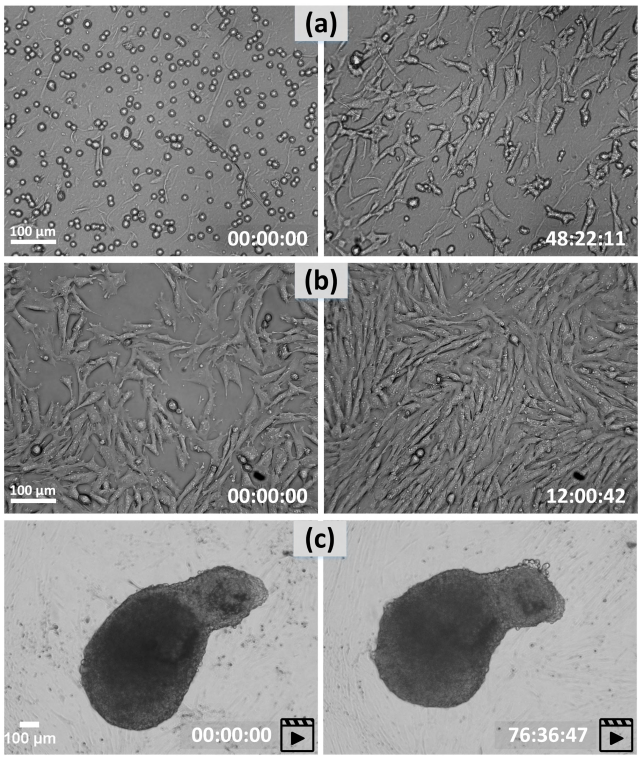

FIGURE 9. Long-term image and video TLM (time- lapse microscopy) with modular microscope in inverted configuration in different contexts. (a) studying the alignment and proliferation capacity of fibroblasts (MEF) on nanocellulose (see Video 1) (b) the spatial and temporal expansion dynamics of fibroblast on glass at various conditions (see Video 2). (c) extended beating monitoring of cardiomyocytes.

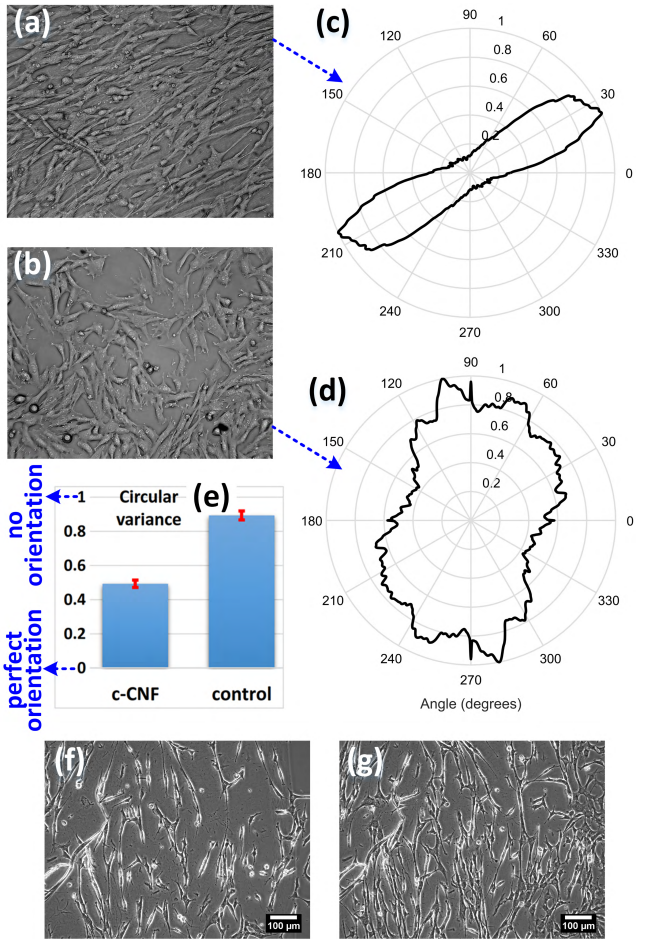

FIGURE 10. Image based orientation analysis of fibroblast (MEF) on cellulose (c-CNF) surfaces using Cytospectre (a,b) Example images of oriented MEF on c-CNF and on control glass surface (showing no dominant orientation). (c,d) Cell orientation plots analysed with Cytospectre. (e) Average circular variance (CV) describing the degree of orientation of cells on cellulose and control plate (f,g) Reference images (20X) captured with a commercial device (Cell-IQ, CM Technologies, Finland) comparable to our system after 24 h and 48 h incubations. With our system, both the cells and cellulose fibres are equally visible and the cell boundaries are comparatively well identifiable.

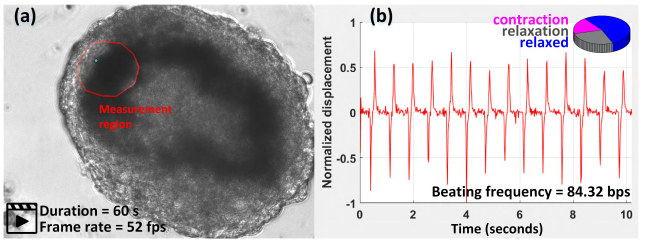

FIGURE 11. (a) Snapshot from the movie of the beating cardiomyocytes on MEA. (b) a 10 s directional beating signal analysed [54] from the region marked by the red polygon with the light blue dot showing the point of reference. The downward peak signifies contraction velocity and the upward peak the relaxation velocity. The inset pie chart: percentage distribution of mechanobiological timing [ms] from the movie analysis. [see also the Video 3 for the full beating profile].

proliferation capacity of MEF on nanocellulose (FIGURE 9a, Video 1), B) the spatial and temporal expansion dynamics of fibroblast on glass at various conditions (FIGURE 9b, Video 2) C) cardiomyocyte (CM) beating behaviour under normal incubation (FIGURE 9c) and hypothermic stressing conditions. The analysis results of A and C are presented in the next two chapters. With the upright microscopy, several simultaneous TLM and sensor logging (cell area temperature, pO_2) were performed. FIGURE 8e shows an example snapshot of a beating cluster on fluorescent pO_2 sensing film from a cardiac hypoxic stressing study. An excerpt from the corresponding pO_2 data log is shown in FIGURE 8f. See [18] for simultaneous pO_2 sensing and CM beating signal analysis from recorded videos using the developed modular system.

1) FIBROBLAST ON CATIONIC CELLULOSE NANOFIBER

In the MEF – TLM study, images were saved in RAW or PNG format (16 bit, camera full resolution [no binning]) and typically at a rate of two images per minute. The TLM program keeps the Illumination off at all times except at times of microscopy logging and during a few seconds of LED stabilization time. The TLM snapshots were later combined into a movie (See Video 1), which showed the temporal and spatial evolution of cells and their alignment in line with the structures of nanocellulose. TLM images (eg. FIGURE 10a) collected at the end of the orientation procedures were analysed with CytoSpectre. No dominating orientation was detected on the control glass surface (FIGURE 10b), and the

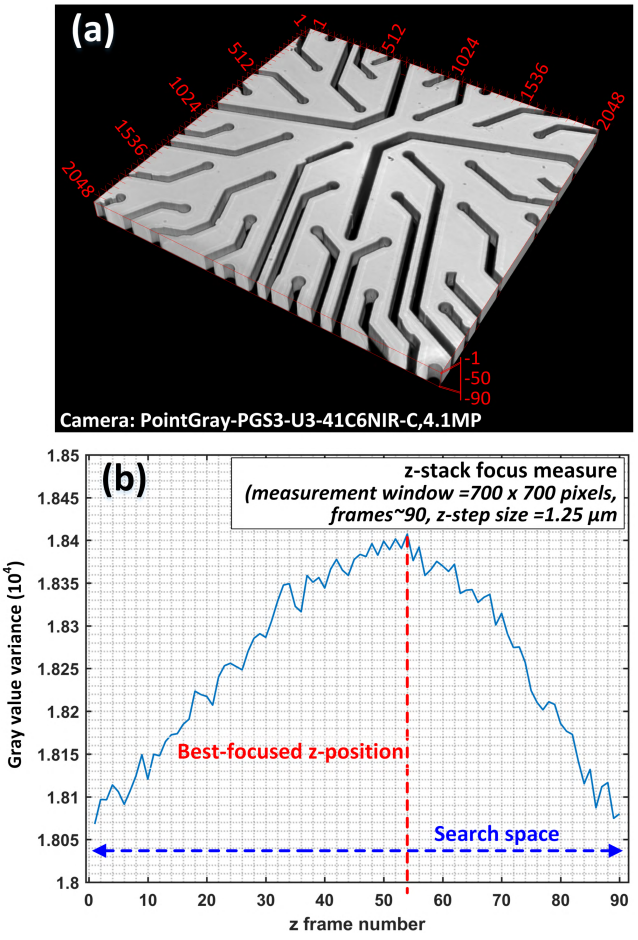

FIGURE 12. Z-stack images (upright) of MEA microelectrode array. (a) A pseudo 3D volume visualization of the stack created with imageJ 3D viewer (b) measurement of focus in the z-stack frames. The red dotted line position shows the best-focused plane where the gray level variance is the highest.

average (three samples) CV computed is 0.92 (FIGURE 10d). On the c-CNF surface (FIGURE 10a), the orientation is clearly visible and the average (eight samples) CV is 0.49 (FIGURE 10c). A similar cell experiment was performed in a commercial long-term live-cell imaging system providing stable incubation at 37°C and 5% CO_2 (Cell-IQ, CM Technologies, Finland). Cells were incubated in Cell-IQ for 48 ± 2 h, while images were recorded. Example images recorded with Cell IQ after 24 h and 48 h are presented for comparison in FIGURE 10f,g. On the contrary, microscopy images with our system show cell boundaries reasonably well and the cells and c-CNF fibres can be visualized better simultaneously.

2) CARDIOMYOCYTES AND VIDEO BASED SIGNAL ANALYSIS

Movies of the beating cardiomyocytes were recorded for TLM durations ranging from a few hours to several days, depending on the objective of the experimental study. Typically, 1-minute movies were recorded once per hour in an 8 bit uncompressed avi format (40-60 fps, 644x480 pixels) and the mechanobiological properties were analysed. A 10-second beating signal analysed from a movie of a CM cluster on MEA (FIGURE 11a) as part of a temperature stressing experiment is shown in FIGURE 11b (see also Video 3). The beating rate is estimated to be 84 beats per minute with average mechanobiological timings 19 ms, 27 ms, 54 ms for contraction, relaxation and relaxed state respectively.

E. Z-STACK ACQUISITION

The z-stack acquisition scheme is also being tested. An example stack of microelectrode array as a pseudo 3D volume (3D viewer/imageJ) is shown in FIGURE 12a. Around 90 frames, each in 1.25 μm step was captured with upright configuration using the 4.1MP camera. In FIGURE 12b, the numerically computed focus from each frame is plotted [56]. The red dotted line indicates the frame with the highest gray level variance corresponding to the best-focused plane in the z search space.

V. DISCUSSION AND CONCLUSION

We present a compact portable live-cell imaging system with a novel architecture and modular sub-assemblies for simultaneous long-term cell imaging, chemical sensing, multisite electrophysiological recording and stimulation. The system has been characterised and tested with histological (stained) and biological live (unstained) specimens. The microscopy performance (resolution and contrast) is comparable to that of traditional phase contrast biological microscopes. Several short and long-term TLM recordings have been performed with neurons, cardiomyocytes and fibroblasts. Successfully completed long-term TLM studies include monitoring the alignment and proliferation of mouse embryonic fibroblasts on nanocellulose, the beating behaviour of human based cardiomyocytes under normal and stressed (hypothermic) environments, and the evaluation of stability and suitability of sensors (temperature sensitive plates, optical pO_2, and pH). Although the imaging unit was developed primarily for our benchtop modular bioreactor, the digital microscope design as such can be used for building custom in-situ microscopes for various applications, where a traditional microscope is not acceptable or affordable. The system is fully functional, and supported with custom software allowing one to control the camera settings and TLM parameters and save the data as independent images or high-fps movies. Further, the software also supports logging data from sensors (temperature, pO_2, pH etc.) connecting via USB and adjusting the ITO-cell heater temperature in real time or in future time points. One major attribute of our system is its invert - upright convertibility, which facilitates a unique set-up for conventional spatiotemporal cell imaging in two directions, and provides flexibility to integrate subassemblies or systems for additional measurement tasks.

Notably, the image plane is reasonably planar without barrel or pincushion distortions. The microscope does not suffer from focusing issues nor display colour halos, evidently owing to the existence of a well-defined image plane without noticeable chromatic and spherical aberrations. This was

partly expected when highly corrected objectives were chosen. Nevertheless, vignetting - the peripheral image darkening [58]- could be a concern, if a camera with a large (>2/3 -inch) sensor is selected or the flange distance is too short in the assembly. For the used cameras', the pixel size (3.75-5 um) is adequate (Nyquist sampling) to preserve the spatial resolution of the objectives since the diffraction Airy disk size of objectives are 23.54 μm (=10X $\times$ 0.61 $\times$ 546 nm/0.1415NA), 23.84 μm and 43 μm for 10X, 20X and 40X, respectively. Enhancing magnification using extension tubes is inexpensive, as it requires no extra optics. They can be mounted without disturbing the objectives, either independently or as a stack of several tubes to produce higher magnification. However, the maximum usable magnification by this approach has a limit, depending on the objective type and NA, beyond which the image looks bigger but the contrast and quality are poor [59]. Calibration of magnification/FOV for each objective - extension tube combination is also necessary, as magnification cannot be directly deduced. This is especially true if the actual scale is to be marked on the captured images. As the objective lenses are implemented slightly differently than in a benchtop microscope, the full advantage of original NA of the objectives gets compromised. However, this enhances the working distance in our system which is advantageous in many instances. Measurements of focus stability and optical flow suggest the system is mechanically stable over tens of hours with a frame support pillar and with a constant heater temperature. However, addressing the focus drift during cell culturing even at a constant temperature is not easy and straightforward especially when the viscosity and refractive index of the culture medium are prone to variations due to evaporation and biochemical changes by the growth and expansion of cells. Currently, manual focus correction is carried out once a day, but it could be automated in future by including a dedicated hardware. A basic z-stack acquisition scheme has been tested, but more experiments using live specimens, and further coding of the data acquisition program is needed for controlling the camera module in the right increments and to synchronize the camera acquisition. If the z-stack acquisition is implemented efficiently with the TLM, it could also be useful for periodically correcting the focus drift as described in [60] without using any dedicated hardware.

Cell culture experiments with integrated MEA amplifier for simultaneous pO_2, electrophysiological recording and TLM are scheduled for later this year. At present, the system is not equipped with vibration mitigation measures. Integrating a benchtop vibration isolation platform would be certainly advantageous for reducing noise and vibrations in high fps movie recordings. The long-term objective of this research is to develop a versatile incubator-independent benchtop bioreactor to automate cell-culture experiments and simultaneously expand its range of possibilities for combined electrical, optical and electrophysiological measurements. Intended applications include *in-vitro* characterization and differentiation of various cell types, chemical measurements and drug screening. A high quality TLM with these studies can undeniably yield an absolute or a more holistic view of the dynamic activity in complex cellular microenvironment.

The ergonomic future-proof system design brings about a further customizable platform for testing diverse optical components and measurement systems. Integration of a non-contact pH measurement module as previously described in [19] and [61] as part of the forthcoming perfusion module or as a completely new CMOS module for 2D pH maps is also under consideration. We envision a widespread application of our digital microscope assembly and portable modular system for long-term *in-vitro* monitoring in various fields of life sciences.

ACKNOWLEDGMENT

We gratefully acknowledge Olli Tanhuanpää, Verho Jarmo, Jouni Niemelä and Antti-Juhana Mäki, Tampere University of Technology, for technical assistance, Panu Lahtinen, VTT Technical Research Centre of Finland Ltd, for providing nanocellulose and Tanja Paavilainen, University of Tampere, for providing neurons for trial imaging.

REFERENCES

[1] S. L. Shorte and F. Frischknecht, *Imaging cellular and molecular biological functions*. Berlin, Germany: Springer-Verlag, 2007.

[2] M. M. Frigault, J. Lacoste, J. L. Swift, and C. M. Brown, "Live-cell microscopy—Tips and tools," *J. Cell Sci.*, vol. 122, no. 6, pp. 753–767, 2009.

[3] Nikon. *Live-Cell Imaging and Perfusion Chambers MicroscopyU*. Accessed: Aug. 1, 2017. [Online]. Available: https://www.microscopyu.com/references/live-cell-imaging-and-perfusion-chambers

[4] Okolab. *Microscope Enclosures*. Accessed: Aug. 1, 2017. [Online]. Available: http://www.oko-lab.com/live-cell-imaging/cage-incubator/temperature-unit

[5] A. G. Godin, B. Lounis, and L. Cognet, "Super-resolution microscopy approaches for live cell imaging," *Biophys. J.*, vol. 107, no. 8, pp. 1777–1784, Oct. 2014.

[6] D. Jin *et al.*, "Compact wireless microscope for *in-situ* time course study of large scale cell dynamics within an incubator," *Sci. Rep.*, vol. 5, Dec. 2015, Art. no. 18483.

[7] Y. S. Zhang *et al.*, "A cost-effective fluorescence mini-microscope for biomedical applications," *Lab Chip*, vol. 15, no. 18, pp. 3661–3669, 2015.

[8] M. B. Esch, T. L. King, and M. L. Shuler, "The role of body-on-a-chip devices in drug and toxicity studies," *Annu. Rev. Biomed. Eng.*, vol. 13, no. 1, pp. 55–72, Aug. 2011.

[9] N. S. Bhise *et al.*, "Organ-on-a-chip platforms for studying drug delivery systems," *J. Control. Release*, vol. 190, pp. 82–93, Sep. 2014.

[10] A. M. Ghaemmaghami, M. J. Hancock, H. Harrington, H. Kaji, and A. Khademhosseini, "Biomimetic tissues on a chip for drug discovery," *Drug Discovery Today*, vol. 17, nos. 3–4, pp. 173–181, 2012.

[11] C. Moraes, G. Mehta, S. C. Lesher-Perez, and S. Takayama, "Organs-on-a-Chip: A focus on compartmentalized microdevices," *Ann. Biomed. Eng.*, vol. 40, no. 6, pp. 1211–1227, Jun. 2012.

[12] D. Huh, G. A. Hamilton, and D. E. Ingber, "From 3D cell culture to organs-on-chips," *Trends Cell Biol.*, vol. 21, no. 12, pp. 745–754, Dec. 2011.

[13] S. N. Bhatia and D. E. Ingber, "Microfluidic organs-on-chips," *Nature Biotechnol.*, vol. 32, no. 8, p. 760, 2014.

[14] Y. Sei, K. Justus, P. LeDuc, and Y. Kim, "Engineering living systems on chips: From cells to human on chips," *Microfluidics Nanofluidics*, vol. 16, no. 5, pp. 907–920, May 2014.

[15] J. P. Wikswo, "The relevance and potential roles of microphysiological systems in biology and medicine," *Exp. Biol. Med.*, vol. 239, no. 9, pp. 1061–1072, 2014.

[16] Š. Selimović, M. R. Dokmeci, and A. Khademhosseini, "Organs-on-a-chip for drug discovery," *Current Opinion Pharmacol.*, vol. 13, no. 5, pp. 829–833, 2013.
[17] M. L. Moya and S. C. George, "Integrating *in vitro* organ-specific function with the microcirculation," *Current Opinion Chem. Eng.*, vol. 3, pp. 102–111, Mar. 2014.
[18] H. Välimäki *et al.*, "Fluorimetric oxygen sensor with an efficient optical read-out for *in vitro* cell models," *Sensors Actuators B, Chem.*, vol. 249, pp. 738–746, Oct. 2017.
[19] D. K. Rajan *et al.*, "Optical non-contact pH measurement in cell culture with sterilizable, modular parts," *Talanta*, vol. 161, pp. 755–761, Dec. 2016.
[20] I. Taurino *et al.*, "Platinum nanopetal-based potassium sensors for acute cell death monitoring," *RCS Adv.*, vol. 6, no. 46, pp. 40517–40526, 2016.
[21] I. Etaluma. *Lumascopes*. Accessed: Aug. 3, 2017. [Online]. Available: http://www.etaluma.com/products/about-lumascope-fluorescent-microscopes/
[22] E. BioScience. (2016). Real-time, quantitative live-cell analysis. IncuCyte ZOOM System. Accessed: Aug. 3, 2017. [Online]. Available: https://www.essenbioscience.com/media/uploads/files/8000-0333-E00-IncuCyte_ZOOM_brochure.pdf
[23] J. H. Jung, C. Han, S. A. Lee, J. Kim, and C. Yang, "Microfluidic-integrated laser-controlled microactuators with on-chip microscopy imaging functionality," *Lab Chip*, vol. 14, no. 19, pp. 3781–3789, 2014.
[24] C. Han, S. Pang, D. V. Bower, P. Yiu, and C. Yang, "Wide field-of-view on-chip Talbot fluorescence microscopy for longitudinal cell culture monitoring from within the incubator," *Anal. Chem.*, vol. 85, no. 4, pp. 2356–2360, Feb. 2013.
[25] G. Zheng, S. A. Lee, Y. Antebi, M. B. Elowitz, and C. Yang, "The ePetri dish, an on-chip cell imaging platform based on subpixel perspective sweeping microscopy (SPSM)," *Proc. Nat. Acad. Sci. USA*, vol. 108, no. 41, pp. 16889–16894, Oct. 2011.
[26] J. El-Ali, P. K. Sorger, and K. F. Jensen, "Cells on chips," *Nature*, vol. 442, no. 7101, pp. 403–411, Jul. 2006.
[27] W. Bishara *et al.*, "Holographic pixel super-resolution in portable lensless on-chip microscopy using a fiber-optic array," *Lab Chip*, vol. 11, no. 7, pp. 1276–1279, Apr. 2011.
[28] A. Greenbaum, U. Sikora, and A. Ozcan, "Field-portable wide-field microscopy of dense samples using multi-height pixel super-resolution based lensfree imaging," *Lab Chip*, vol. 12, no. 7, pp. 1242–1245, Apr. 2012.
[29] W. Bishara, T.-W. Su, A. F. Coskun, and A. Ozcan, "Lensfree on-chip microscopy over a wide field-of-view using pixel super-resolution," *Opt. Exp.*, vol. 18, no. 11, pp. 11181–11191, May 2010.
[30] Z. F. Phillips, M. Chen, and L. Waller, "Single-shot quantitative phase microscopy with color-multiplexed differential phase contrast (cDPC)," *PLoS ONE*, vol. 12, no. 2, p. e0171228, Feb. 2017.
[31] A. Ozcan and E. McLeod, "Lensless imaging and sensing," *Annu. Rev. Biomed. Eng.*, vol. 18, no. 1, pp. 77–102, Jul. 2016.
[32] A. Greenbaum *et al.*, "Imaging without lenses: achievements and remaining challenges of wide-field on-chip microscopy," *Nature Methods*, vol. 9, no. 9, pp. 889–895, 2012.
[33] B. A. Flusberg, E. D. Cocker, W. Piyawattanametha, J. C. Jung, E. L. M. Cheung, and M. J. Schnitzer, "Fiber-optic fluorescence imaging," *Nature Methods*, vol. 2, no. 12, pp. 941–950, Dec. 2005.
[34] M. Pierce, D. Yu, and R. Richards-Kortum, "High-resolution fiber-optic microendoscopy for *in situ* cellular imaging," *J. Vis. Exp.*, vol. 47, p. e2306, Jan. 2011.
[35] D. Shin, M. C. Pierce, A. M. Gillenwater, M. D. Williams, and R. R. Richards-Kortum, "A fiber-optic fluorescence microscope using a consumer-grade digital camera for *in vivo* cellular imaging," *PLoS ONE*, vol. 5, no. 6, p. e11218, Jun. 2010.
[36] F. Helmchen, "Miniaturization of fluorescence microscopes using fibre optics," *Experim. Physiol.*, vol. 87, no. 6, pp. 737–745, Nov. 2002.
[37] K.-B. Sung, C. Liang, M. Descour, T. Collier, M. Follen, and R. Richards-Kortum, "Fiber-optic confocal reflectance microscope with miniature objective for *in vivo* imaging of human tissues," *IEEE Trans. Biomed. Eng.*, vol. 49, no. 10, pp. 1168–1172, Oct. 2002.
[38] Y. Ando *et al.*, "*In vivo* bioluminescence and reflectance imaging of multiple organs in bioluminescence reporter mice by bundled-fiber-coupled microscopy," *Biomed. Opt. Exp.*, vol. 7, no. 3, pp. 963–978, 2016.
[39] X. Meng *et al.*, "Smartphone based hand-held quantitative phase microscope using the transport of intensity equation method," *Lab Chip*, vol. 17, no. 1, pp. 104–109, 2017.
[40] A. Skandarajah, C. D. Reber, N. A. Switz, and D. A. Fletcher, "Quantitative imaging with a mobile phone microscope," *PLoS ONE*, vol. 9, no. 5, p. e96906, 2014.
[41] Y. S. Zhang *et al.*, "Hybrid microscopy: Enabling inexpensive high-performance imaging through combined physical and optical magnifications," *Sci. Rep.*, vol. 6, Mar. 2016, Art. no. 22691.
[42] M. P. Walzik *et al.*, "A portable low-cost long-term live-cell imaging platform for biomedical research and education," *Biosens. Bioelectron.*, vol. 64, pp. 639–649, Feb. 2015.
[43] G. O. F. Parikesit, M. Darmawan, and A. Faisal, "Quantitative low-cost webcam-based microscopy," *Opt. Eng.*, vol. 49, no. 11, p. 113205, Nov. 2010.
[44] J. Kreutzer *et al.*, "Structured PDMS chambers for enhanced human neuronal cell activity on MEA platforms," *J. Bionic Eng.*, vol. 9, no. 1, pp. 1–10, Mar. 2012.
[45] J. Kreutzer, L. Ylä-Outinen, A. J. Mäki, M. Ristola, S. Narkilahti, and P. Kallio, "Cell culture chamber with gas supply for prolonged recording of human neuronal cells on microelectrode array," *J. Neurosci. Methods*, vol. 280, pp. 27–35, Mar. 2017.
[46] D. B. Murphy, *Fundamentals of Light Microscopy and Electronic Imaging*, vol. 53. Hoboken, NJ, USA: Wiley, 2012.
[47] J. R. Lakowicz, *Principles of Fluorescence Spectroscopy*, 3rd ed. New York, NY, USA: Springer, 2006.
[48] D. Georg. *Camera GUI (Version 1.0)*. Accessed: Aug. 1, 2017. [Online]. Available: https://se.mathworks.com/matlabcentral/fileexchange/35919-cameragui
[49] MathWorks MATLAB Hardware Team. (2014). *MATLAB Support Package for Arduino Hardware (Version 1.1), MATLAB Central File Exchange*. Accessed: Apr. 1, 2014. [Online]. Available: https://se.mathworks.com/matlabcentral/fileexchange/47522-matlab-support-package-for-arduino-hardware
[50] MathWorks Image Acquisition Toolbox Team. *Image Acquisition Toolbox Support Package for Point Grey Hardware (Version 1.1)*. Accessed: Aug. 1, 2017. [Online]. Available: https://se.mathworks.com/matlabcentral/fileexchange/45178-image-acquisition-toolbox-support-package-for-point-grey-hardware
[51] A. Skogberg, A.-J. Mäki, P. Lahtinen, and P. Kallio, "Cellulose nanofiber alignment using evaporation-induced droplet-casting, and cell alignment on aligned nanocellulose surfaces," *Biomacromolecules*, vol. 18, no. 12, pp. 3936–3953, 2017.
[52] A. L. Lahti *et al.*, "Model for long QT syndrome type 2 using human iPS cells demonstrates arrhythmogenic characteristics in cell culture," *Disease Models Mech.*, vol. 5, no. 2, pp. 220–230, Mar. 2012.
[53] K. Kartasalo *et al.*, "CytoSpectre: A tool for spectral analysis of oriented structures on cellular and subcellular levels," *BMC Bioinf.*, vol. 16, no. 1, p. 344, Dec. 2015.
[54] A. Ahola, A. Kiviaho, K. Larsson, M. Honkanen, K. Aalto-Setälä, and J.Hyttinen, "Video image-based analysis of single human induced pluripotent stem cell derived cardiomyocyte beating dynamics using digital image correlation," *Biomed. Eng. Online*, vol. 13, no. 1, p. 39, 2014.
[55] I. T. Young, R. Zagers, L. J. van Vliet, J. Mullikin, F. Boddeke, and H. Netten, "Depth-of-focus in microscopy," in *Proc. 8th Scandin. Conf. Image Anal.*, 1993, pp. 493–498.
[56] S. Pertuz, D. Puig, and M. A. Garcia, "Analysis of focus measure operators for shape-from-focus," *Pattern Recognit.*, vol. 46, no. 5, pp. 1415–1432, 2013.
[57] Y. David. (2010). *Affine Optic Flow (Version 1.3), MATLAB Central File Exchange*. Accessed: Mar. 3, 2017. [Online]. Available: https://se.mathworks.com/matlabcentral/fileexchange/27093-affine-optic-flow?focused=6019470&tab=example
[58] F. J. W.-M. Leong, M. Brady, and J. O. D. McGee, "Correction of uneven illumination (vignetting) in digital microscopy images," *J. Clin. Pathol.*, vol. 56, no. 8, pp. 619–621, Aug. 2003.
[59] Nikon. *Useful Magnification Range MicroscopyU*.Accessed: Aug. 10, 2017. https://www.microscopyu.com/microscopy-basics/useful-magnification-range
[60] M. Kreft, M. Stenovec, and R. Zorec, "Focus-drift correction in time-lapse confocal imaging," *Ann. New York Acad. Sci.*, vol. 1048, no. 1, pp. 321–330, Jun. 2005.
[61] D. K. Rajan *et al.*, "Monitoring pH, temperature and humidity in long-term stem cell culture in CO2 incubator," in *Proc. IEEE Int. Symp. Med. Meas. Appl. (MeMeA)*, May 2017, pp. 470–474.

DHANESH KATTIPPARAMBIL RAJAN received the M.Sc. degree (Tech.) in biomedical engineering from the Tampere University of Technology (TUT), Finland, in 2008, where he is currently pursuing the D.Sc. degree with BioMediTech Institute. He was with the photolithography facility at TUT for four years. He is currently a Research Scientist with BioMediTech Institute and the Faculty of Biomedical Sciences and Engineering, TUT, where he develops compact-modular imaging and optical measurement techniques and systems.

JOOSE KREUTZER received the B.Eng. degree in electrical and electronic engineering from the University of Sunderland, Sunderland, U.K., in 2003, and the M.Sc. degree in electrical engineering from the Tampere University of Technology (TUT), Tampere, Finland, in 2005. He is currently a Research Scientist with the Micro and Nanosystems Research Group, BioMediTech Institute, and the Faculty of Biomedical Sciences and Engineering, TUT. His current research interests include microfabrication, microfluidics, and their applications in biomedical engineering, especially for stem cell-based bioengineering.

HANNU VÄLIMÄKI received the M.Sc. degree in electrical engineering from the Tampere University of Technology (TUT), Tampere, Finland, in 1996. He was a Research Scientist in the field of acoustical and optical sensors with the VTT Technical Research Centre of Finland, Tampere, until 2013. He is currently with the BioMediTech Institute and Faculty of Biomedical Sciences and Engineering, TUT, where he develops optical sensing technologies for cell culturing applications.

MARI PEKKANEN-MATTILA received the Ph.D. degree in stem cell and tissue engineering from the University of Tampere, Finland, in 2011. Her research interests include human induced pluripotent stem cells, cell differentiation, and disease modeling of human genetic cardiac diseases.

ANTTI AHOLA received the master's degree in biomedical engineering from the Tampere University of Technology, Finland, in 2010. He is currently pursuing the D.Sc. degree. His research interests include cardiomyocyte biomechanics, video microscopy, and image analysis.

ANNE SKOGBERG received the master's degree in cell and tissue engineering from the University of Tampere, Finland, in 2010. She is currently pursuing the Ph.D. degree with the Tampere University of Technology, Finland. Her research interests include nanocellulose and its utilization in biomedical applications.

KATRIINA AALTO-SETÄLÄ received the M.D. degree. She is currently a Professor of physiology with the Faculty of Medicine and Life Sciences, University of Tampere, and a Cardiologist with the Heart Hospital, Tampere University Hospital, Finland. She is an Invasive Cardiologist and is in charge of the Genetic Cardiac Outpatient Clinic, Heart Hospital. She was involved in human genetic cardiac diseases, such as genetic arrhythmias and atherosclerosis with the help of induced pluripotent stem cell technology. The main aim of the research group is to learn more about the basic pathology of the genetic diseases as well as to test current and new pharmaceutical agents to correct the abnormalities. Her research group in collaboration with researchers at the Tampere University of Technology has also invented new methods to monitor and analyze the maturity and functionality of cardiomyocytes.

HEIMO IHALAINEN started teaching measurement technology at the Tampere University of Technology in 1974, and conducted research in multivariate signals in the 1990s. In 2000, he was involved in a new topic, measurement based on images, and though he is officially retired now, the topic motivates him to continue in the field.

PASI KALLIO received the M.S. degree in electrical engineering and the D.Tech. degree in automation engineering from the Tampere University of Technology (TUT), Tampere, Finland, in 1994 and 2002, respectively. Since 2008, he has been a Professor of automation engineering at TUT. He is currently the Vice Director of the Faculty of Biomedical Sciences and Engineering. He has authored over 130 articles and has over ten patent applications. His current research interests include microrobotics, microfluidics, and their automation in cell and tissue engineering, medical diagnostics, and soft material testing applications. He was a recipient of the Finnish Automation Society Award in 2009. He was the Chair of the IEEE Finland Section from 2012 to 2013.

JUKKA LEKKALA received the M.Sc. degree in electronics and the D.Sc. (Tech.) degree in biomedical engineering from the Tampere University of Technology (TUT), Tampere, Finland, in 1979 and 1984, respectively. From 1985 to 2001, he was a Senior Research Scientist with the VTT Technical Research Centre of Finland in different research units developing biosensor technology and sensor materials. In 1991, he was appointed as a Docent of bioelectronics with the University of Oulu and a Docent of biomedical engineering at TUT. Since 2002, he has been a Professor of automation engineering at TUT. He is currently a Professor Emeritus with the Faculty of Biomedical Sciences and Engineering (TUT-BMT). He has over 170 scientific publications and ten patents. His research interests include sensors, measurement systems, and biosensing.